Molecular Therapy
Nucleic Acids
Original Article

MicroRNA miR-29b regulates diabetic aortic remodeling and stiffening

Isabel N. Schellinger,[1,2,3] Markus Wagenhäuser,[4] Giriprakash Chodisetti,[1] Karin Mattern,[1] Angelika Dannert,[1] Anne Petzold,[1] Joanna Jakubizka-Smorag,[1] Fabian Emrich,[5,6] Josephina Haunschild,[6] Andreas Schuster,[1,2] Elisabeth Schwob,[7] Kei Schulz,[7] Lars Maegdefessel,[8,9] Joshua M. Spin,[10,11] Michael Stumvoll,[3] Gerd Hasenfuß,[1,2] Philip S. Tsao,[10,11] and Uwe Raaz[1,2]

[1]Department of Cardiology and Pneumology, Heart Center at the University Medical Center Göttingen, Göttingen, Germany; [2]German Center for Cardiovascular Research (DZHK) e.V., Partner site Göttingen, Göttingen, Germany; [3]Department for Endocrinology, Nephrology and Rheumatology, University Medical Center Leipzig, University of Leipzig, Leipzig, Germany; [4]Department of Vascular and Endovascular Surgery, University Hospital Düsseldorf, Heinrich-Heine-University, Düsseldorf, Germany; [5]Department of Cardiothoracic and Vascular Surgery, Goethe University Hospital Frankfurt, Frankfurt, Germany; [6]Department of Cardiac Surgery, Heart Center Leipzig, Leipzig, Germany; [7]Department of Anesthesiology, University Medical Center Göttingen, Göttingen, Germany; [8]Department for Vascular and Endovascular Surgery, Klinikum rechts der Isar der Technischen Universität München, Munich, Germany; [9]Karolinska Institute, Department of Medicine, Stockholm, Sweden; [10]Division of Cardiovascular Medicine, Stanford University School of Medicine, Stanford, CA, USA; [11]VA Palo Alto Health Care System, Palo Alto, CA, USA

Patients with type 2 diabetes (T2D) are threatened by excessive cardiovascular morbidity and mortality. While accelerated arterial stiffening may represent a critical mechanistic factor driving cardiovascular risk in T2D, specific therapies to contain the underlying diabetic arterial remodeling have been elusive. The present translational study investigates the role of microRNA-29b (miR-29b) as a driver and therapeutic target of diabetic aortic remodeling and stiffening. Using a murine model (db/db mice), as well as human aortic tissue samples, we find that diabetic aortic remodeling and stiffening is associated with medial fibrosis, as well as fragmentation of aortic elastic layers. miR-29b is significantly downregulated in T2D and miR-29b repression is sufficient to induce both aortic medial fibrosis and elastin breakdown through upregulation of its direct target genes *COL1A1* and *MMP2* thereby increasing aortic stiffness. Moreover, antioxidant treatment restores aortic miR-29b levels and counteracts diabetic aortic remodeling. Concluding, we identify miR-29b as a comprehensive—and therefore powerful—regulator of aortic remodeling and stiffening in T2D that moreover qualifies as a (redox-sensitive) target for therapeutic intervention.

INTRODUCTION

Type 2 diabetes (T2D) is a spreading worldwide epidemic. In 2010, an estimated 285 million adults were affected, and this number is believed to rise to 439 million by 2030. T2D is linked to dramatically increased cardiovascular risk. A wide range of cardiovascular diseases, including myocardial infarction, stroke, hypertension, and diabetic cardiomyopathy contribute to the worsened quality-of-life, morbidity, and mortality observed in T2D patients.[1,2]

Increased arterial stiffness is a frequently overlooked phenomenon in T2D that may represent a critical mechanistic link to its deleterious cardiovascular complications.[3,4] Stiff conduit arteries (such as the aorta) lose their capability to mechanically buffer the pulsatile cardiac ejections (i.e., reduced Windkessel function), which results in widespread augmented hemodynamic stress and end-organ damage (notably to the brain, heart, or kidneys).[5] As such, arterial stiffness has been identified as a strong independent cardiovascular risk factor.[6]

Unfortunately, specific therapies to reduce diabetic vascular stiffening and potentially forestall the resulting cardiovascular harm have been elusive to date. This may partly be due to the complex mechanisms involved in diabetic arterial stiffening including vascular fibrosis and elastic tissue destruction.[5]

The discovery of non-coding microRNAs (miRNAs or miRs) has provided new opportunities for innovative therapeutic approaches. miRNAs are small, single-stranded, noncoding RNA molecules, usually about 22 nucleotides in length, that regulate gene expression through repression of target mRNA translation.[7] Importantly, through inhibition of multiple target genes, a single miRNA may simultaneously modulate multiple signaling pathways and complex biological processes. Thus, miRNAs may be ideally suited to orchestrate arterial stiffening in diabetes.

In particular, miR-29b has been identified as a diverse regulator of extracellular matrix (ECM) genes.[8] The present study investigates the role of miR-29b as a potential regulator and therapeutic target in diabetic arterial stiffening.

Received 18 August 2020; accepted 19 February 2021;
https://doi.org/10.1016/j.omtn.2021.02.021.

Correspondence: Uwe Raaz, MD, Department of Cardiology and Pneumology, Center at the University Medical Center Göttingen, Göttingen, Germany.
E-mail: uwe.raaz@med.uni-goettingen.de

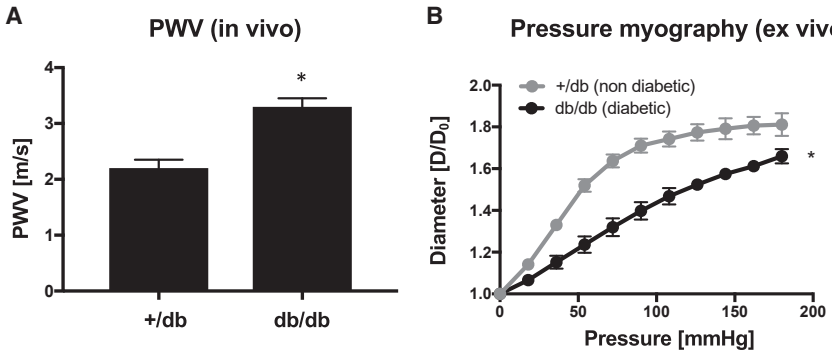

Figure 1. db/db mice exhibit increased pulse-wave velocity (PWV) and structural aortic stiffness

(A) PWV measurement in diabetic db/db mice versus non-diabetic controls (+/db mice). Values are mean ± SEM. *p < 0.05 versus +/db controls (n = 5/group). (B) Aortic pressure diameter curves from db/db mice versus +/db controls. Values are mean ± SEM. *p < 0.05 versus +/db controls. (n = 5/group).

RESULTS

Aortic stiffness is increased in diabetic mice

To investigate the impact of the diabetic metabolic state on arterial stiffness, we employed an established diabetic (db/db) mouse model. Measuring pulse-wave velocity (PWV; Figure 1A), the clinical gold standard parameter to quantify arterial stiffness *in vivo*, we found that 10-week-old db/db mice exhibit significantly increased PWV compared to nondiabetic +/db controls. Further, to discern whether increased aortic stiffness in db/db mice is due to increased structural stiffness of the aortic wall, we performed *ex vivo* pressure myography. Thoracic aortic segments taken from db/db mice exhibited significantly increased "material" stiffness of the explanted tissue (compared to +/db controls; Figure 1B).

Diabetic aortae exhibit medial fibrosis and elastin fragmentation

Collagen abundance and the integrity of the elastic layers in the arterial media both contribute to structural arterial stiffness. Accordingly, we next focused on these ECM characteristics as a potential basis for the observed aortic stiffening in db/db mice. Histological examinations revealed increased fibrosis and collagen I expression in the media from db/db aortae compared to controls (Figures 2A and 2B). Additionally, we detected marked elastin fragmentation in diabetic db/db aortae (Figures 2A and 2C). As elastin digestion may result from increased enzymatic activity, we assessed the elastolytic activity in aortic sections via *in situ* zymography. Aortic sections from db/db mice exhibited markedly higher elastolytic enzyme activity than +/db controls (Figure 2A). This phenomenon was associated with increased vascular expression of the elastolytic matrix metalloproteinase Mmp2 in diabetic aortae (Figure 2A).

To validate the translational relevance of these findings, we analyzed thoracic aortic tissue samples from diabetic and non-diabetic patients that were collected during open surgery. We also found increased collagen I deposition and elastin fragmentation in aortae from diabetic patients (Figures 2D and 2E).

miR-29b is downregulated, with de-repression of pro-fibrotic and elastolytic target genes in diabetic aortae

We sought to investigate the molecular mechanisms involved in the structural aortic remodeling leading to increased arterial stiffness in T2D, focusing on miR-29b, a known upstream regulator of both fibrosis and elastolysis. In fact, miR-29b expression was significantly downregulated in db/db thoracic aortic tissue (Figure 3A). *In situ* hybridization (ISH) revealed that miR-29b downregulation occurred primarily in the aortic media (vascular smooth muscle [VSM] layer; Figure 3B). This downregulation of miR-29b was associated with substantially increased expression of miR-29b-target genes *Col1a1*, as well as *Mmp2* (Figure 3C). Expression analyses in T2D human aortic tissue confirmed downregulation of miR-29b, as well as upregulation of *COL1A1* and *MMP2*.

Inhibition of miR-29b induces a "diabetic" aortic phenotype and increases arterial stiffness in non-diabetic mice

To further elucidate the mechanistic significance of miR29-depletion for aortic structure and function, we tested the effects of pharmacologic miR-29b inhibition *in vivo* using a specific miR-29b inhibitor (anti-miR-29b). Following systemic injection in non-diabetic +/db mice, we were able to detect fluorescently labeled anti-miR-29b modulator enrichment in the aortic wall (Figure S1). On a gene-expression level, this intervention induced a significant de-repression (upregulation) of miR-29b target genes *Col1a1* and *Mmp2* in +/db aortae (Figures 4A and 4B). Structurally, this was accompanied by increased medial collagen expression (Figures 4B and 4C) and elastolytic activity (Figures 4B and 4D) resulting in significant elastin fragmentation—quite similar to the aortic phenotype found in diabetic db/db mice (Figure 2A). Of note, anti-miR-29b treatment did not alter blood glucose levels in non-diabetic +/db mice (Figure S2). Functionally, aortic structural remodeling due to forced miR-29b downregulation resulted in increased aortic stiffness as indicated by *ex vivo* pressure myography (Figure 4E) and *in vivo* PWV quantification (Figure 4F).

miR-29b expression is downregulated under high glucose conditions in human aortic smooth muscle cells and modulates matrix gene expression

Having observed repression of miR-29b in diabetic aortae, we next investigated this phenomenon *in vitro*. Given that downregulation of miR-29b expression was isolated to the aortic medial layer (Figure 3B), we focused on VSM cells (VSMCs), which represent the primary cellular component of this compartment. Exposure of human aortic SMCs (AoSMCs) to high glucose conditions resulted in both downregulation of miR-29b, as well as upregulation of *COL1A1* and *MMP2* (Figure 5A). Treatment of AoSMCs with a miR-29b mimic

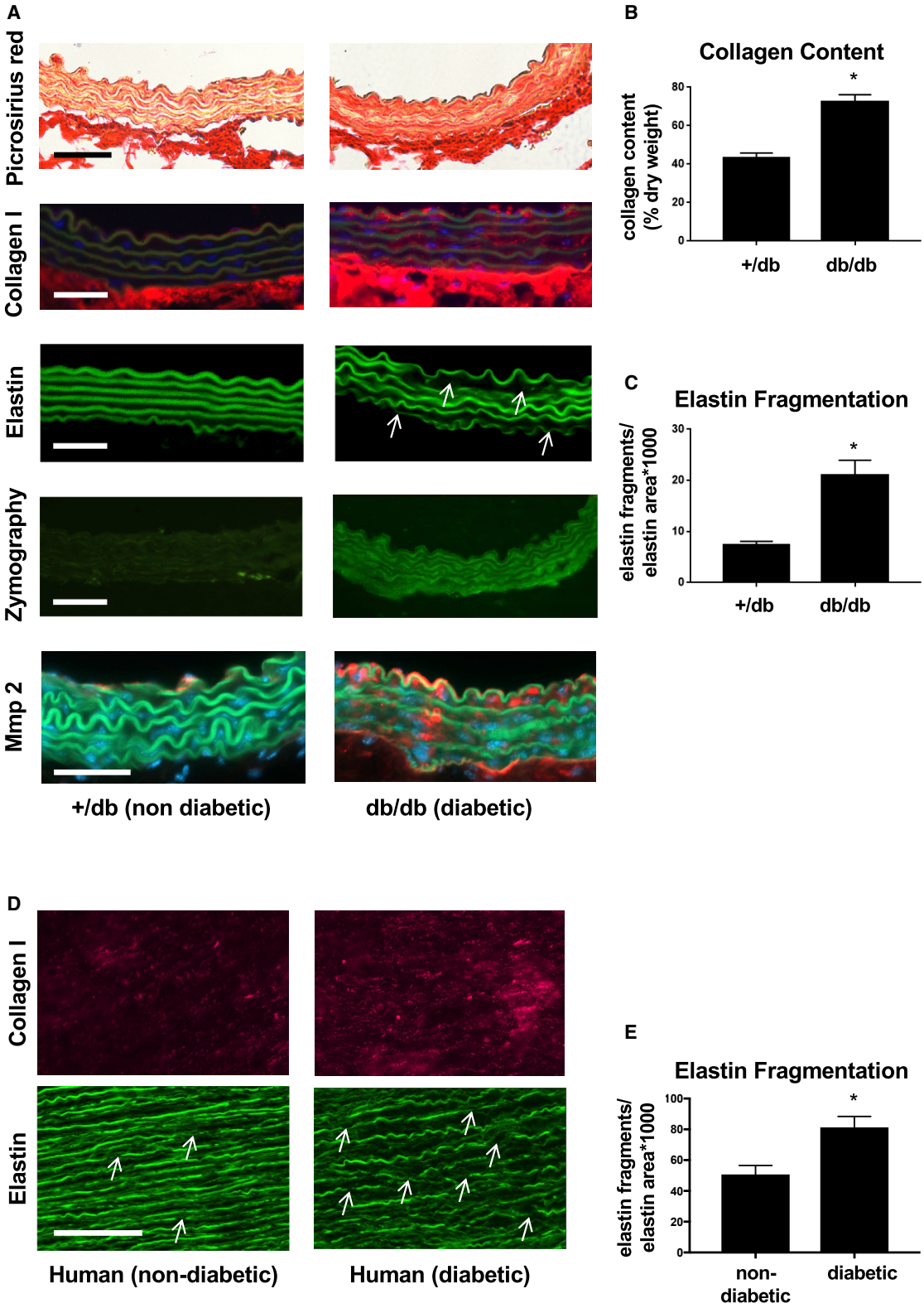

(legend on next page)

repressed *COL1A1* and *MMP2* (Figure 5C) while miR-29b inhibition de-repressed those genes (Figure 5B), further confirming the role of miR-29b as a mechanistic regulator. Moreover, experimental miR-29b modulation was sufficient to induce collagen I and MMP-2 protein expression by AoSMCs under normal glucose conditions and repress those proteins despite high glucose treatment (Figures 5D and 5E).

Antioxidant intervention restores aortic miR-29b expression and prevents aortic remodeling and stiffening in diabetic mice

Having established miR-29b as a regulator of aortic remodeling and stiffening in diabetes, we further investigated potential mechanisms of miR-29b repression in diabetic aortae. Low-grade chronic inflammation and increased oxidative stress are prominent features of the diabetic vasculature. We therefore speculated that miR-29b may be a redox-sensitive target, downregulated by increased reactive oxygen species (ROS). To test this hypothesis, we treated db/db with the antioxidant agent TEMPOL (4-hydroxy-2,2,6,6- tetramethylpiperidine 1-oxyl) between 10 and 20 weeks of age. TEMPOL treatment resulted in a significant decrease in aortic oxidative stress as indicated via *in situ* dihydroethidium (DHE) staining (Figures 6A and 6B) and aortic oxidized ethidium (Oxy-E) high-performance liquid chromatography (HPLC) analysis (Figure 6C). Further, TEMPOL significantly increased aortic miR-29b expression in db/db mice (Figure 6D). This was accompanied by downregulation of ECM target genes *Col1a1* and *Mmp2* (Figure 6E). Structurally, this translated into decreased collagen deposition, as well as reduced Mmp2 abundance and fewer elastin breaks, in the aortic media of TEMPOL-treated db/db mice (Figures 6F–6H). Functionally, TEMPOL counteracted passive aortic stiffening as monitored by pressure myography (Figure 6I) and PWV (Figure 6J).

DISCUSSION

Increasing arterial stiffness is typically observed as a manifestation of arterial aging and has been identified as an independent risk factor for cardiovascular diseases.[9]

The clinical impact of aortic stiffening arises out of both systemic and local vascular effects.[5] Systemically, a stiff aorta fails to buffer the cyclic rise and fall of arterial blood pressure levels (i.e., systolic and diastolic blood pressure) arising out of the pulsatile cardiac ejections. This may result in increased systolic pressure, decreased diastolic pressure, and augmented pulse (systolic-diastolic) pressure levels. While increased systolic and pulse pressure may impose direct mechanical damage to end-organs that critically require high blood flow and therefore have little protective vascular resistance (e.g., brain and kidneys), decreased diastolic blood pressure in particular may impede cardiac perfusion and therefore promote heart failure. Locally, heterogeneous stiffening of aortic segments has been demonstrated to induce stiffness gradients and biomechanical stress favoring aneurysm development.[10]

Arterial stiffening may be accelerated by a variety of diseases, most notably T2D.[5] Indeed, arterial stiffness predicts the development of cardiovascular diseases (CVD) and mortality in patients with T2D, suggesting that diabetes rapidly accelerates vascular "age" leading to augmented cardiovascular morbidity and mortality.

Despite this growing body of evidence, specific interventions to limit diabetic arterial stiffening have not been identified. This may be due to the complex nature of arterial remodeling resulting in increased vascular stiffness. Elastin and collagen represent the major structural components of the arterial ECM and critically define vascular biomechanical characteristics.[11,12] As such, both increased collagen deposition and destruction of the elastic lamellae in the medial layer are major factors contributing to arterial stiffening.[5] Effective anti-stiffness therapies are required to comprehensively address both pathomechanisms. Since miRNAs act as molecular regulators that simultaneously govern multiple downstream target genes, they offer powerful targets for therapeutic modulation.

Here we report that miR-29b is downregulated in human and murine diabetic aortae and that miR-29b repression is a mechanistic driver of collagen deposition and elastin fragmentation, inducing arterial stiffening. Further, we find that miR-29b acts as a redox-sensitive target in diabetic aortae and that antioxidant intervention counteracts diabetic aortic remodeling and stiffening.

Similar to our previous studies, we demonstrated that diabetic db/db exhibit increased structural stiffness of the aortic wall (by pressure myography).[13] We additionally found that this translated into increased PWV *in vivo*, with PWV being the clinical gold standard and prognostically most relevant marker of arterial stiffness[5] (Figure 1).

Focusing further on the structural basis of arterial stiffening in db/db mice, our histologic analyses revealed both marked fibrotic remodeling and elastin fragmentation in the medial layer of diabetic aortae (Figure 2). From a translational perspective, this pattern of aortic ECM remodeling was also observed in human diabetic aortae (Figure 2D), consistent with previous reports.[13–17]

Figure 2. Diabetic aortae exhibit medial fibrosis, increased elastin fragmentation, Mmp2 expression, and activity

(A) Representative images of aortic cross sections from 20-week-old mice stained for collagen via picrosirius red (red = collagen) and anti-collagen I immunofluorescence antibody (red = collagen), elastin (autofluorescence of green elastic lamella; arrows exemplarily indicate thinning and breaks), Mmp2 (red), and elastolytic activity (*in situ* zymography). Original magnifications are 400×. Scale bar represents 50 μm. (B) Total collagen content per aortic dry weight. n = 5/group. Values are mean ± SEM. *p < 0.05 versus +/db control. (C) Elastin fragmentation index quantified from 3 high-power fields of 5 different aortas per group. Values are mean ± SEM. *p < 0.05 versus +/db control (D) Representative images of human aortic sections stained for collagen via anti-collagen I immunofluorescence antibody, and for elastin (via autofluorescence of the elastic lamella; arrows exemplarily indicate thinning and breaks). Original magnifications are 400×. Scale bar represents 100 μm. (E) Elastin fragmentation index quantified from 3 high-power fields of 5 different aortas per group. Values are mean ± SEM. *p < 0.05 versus non-diabetic.

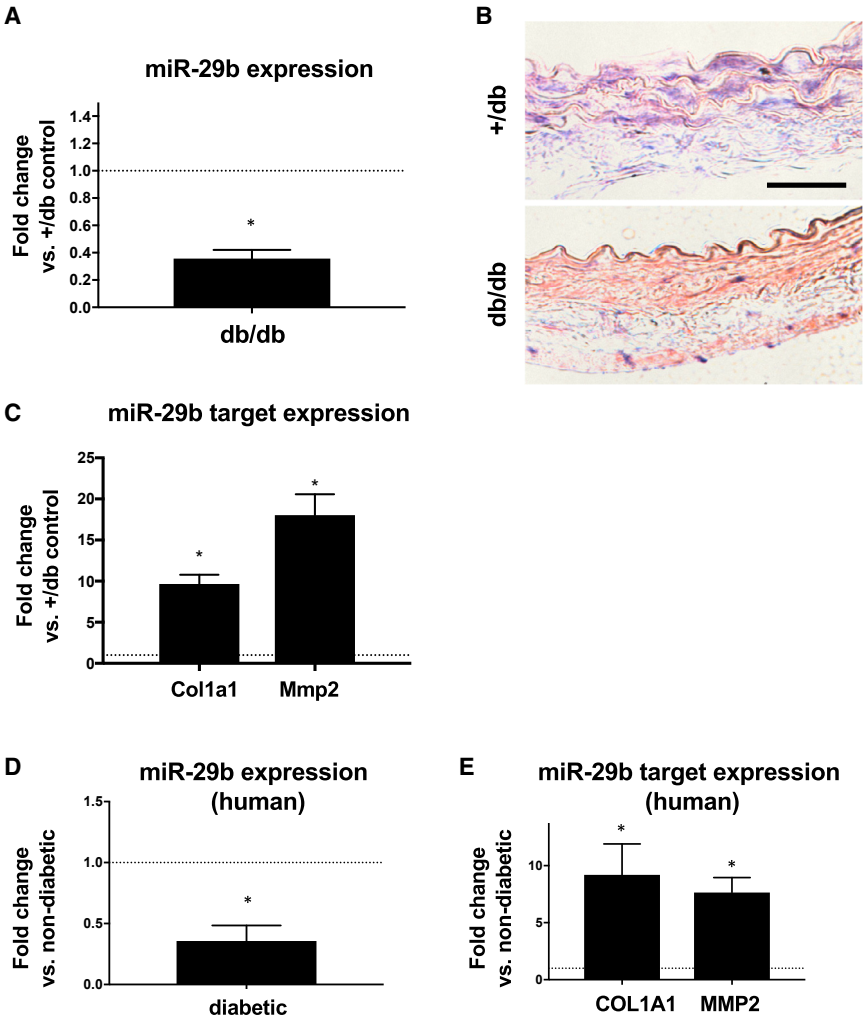

Figure 3. Diabetic aortae show reduced levels of miR-29b and elevated miR29b target genes

(A) miR-29b expression levels in thoracic aortae of db/db mice compared to +/db controls. Values are mean ± SEM and expressed as fold change relative to the mean expression level in +/db controls (=1; dotted line). *p < 0.05 versus +/db. n = 5/group. (B) *In situ* hybridization (ISH) for miR-29b (purple-blue dye) and red nuclear counterstain in the +/db and db/db aortae from 20-week-old mice (original magnification ×400; scale bar, 50 μm). (C) Aortic expression levels of miR-29b target genes *Col1a1* and *Mmp2* in db/db mice compared to +/db controls. Values are mean ± SEM and expressed as fold change relative to the mean expression level in +/db controls (=1; dotted line). *p < 0.05 versus +/db (n = 5/group). (D) miR-29b expression levels in thoracic aortae of diabetic patients (n = 8) compared to non-diabetic patients (n = 8). Values are mean ± SEM and expressed as fold change relative to the mean expression level in non-diabetic patients (=1; dotted line). *p < 0.05 versus non-diabetic patients. (E) Aortic expression levels of miR-29b target genes *COL1A1* and *MMP2* in diabetic patients (n = 8) compared to non-diabetic patients (n = 8). Values are mean ± SEM and expressed as fold change relative to the mean expression level in non-diabetic patients (=1; dotted line). *p < 0.05 versus non-diabetic patients.

While we found increased medial collagen I protein expression as a mechanism leading to diabetic vascular fibrosis, we also detected increased elastolytic activity in db/db aortae facilitating observed fragmentation of elastic layers. Among the heterogenous family of matrix metalloproteinases, MMP-2 is constitutively expressed in VSMCs and exhibits elastin degrading activity that is known to contribute to vascular remodeling and stiffening.[15,18] Accordingly, we found that Mmp-2 expression significantly increased in db/db aortae.

miR-29b dysregulation has been linked to fibrotic remodeling processes in various diseases including myocardial infarction, kidney injury, and abdominal aortic aneurysm (AAA).[19–21] Moreover, many matrix modulating genes including *COL1A1* and *MMP2* belong to the set of directly regulated miR-29b targets.[21,22] This prompted us to investigate the potential impact of miR-29b on diabetic aortic stiffening. Indeed, we found significant miR-29b repression in the medial layer of diabetic db/db aortae alongside increased gene expression of *Col1a1* and *Mmp2*. Importantly from a translational perspective, we also detected an analogous regulation pattern in diabetic human aortic tissue (Figure 3). Downregulation of miR-29b levels has also been observed in blood plasma from patients with T2D, as well as in kidneys from db/db mice, driving diabetic nephropathy.[20,23]

Paradoxically, despite its well-established role as a major cardiovascular risk factor, diabetes mellitus has been identified as a protective factor in AA diseases.[24] We previously found that miR-29b is downregulated in both preclinical models of AAAs as well in human AAA tissue samples.[21] Of note, forced downregulation of miR-29b conveyed a protective effect in AAA models through induction of profibrotic mechanisms.[21] Thus, repression of miR-29b in AAAs may represent a local compensatory mechanism to contain aneurysm growth. In the light of those findings, the observed aortic downregulation of miR-29b levels in diabetic conditions may constitute a molecular mechanistic link toward AA protection found in patients with diabetes mellitus.

To further explore the mechanistic role of miR-29b dysregulation as a driver of arterial stiffening, we generated a mouse model of forced miR-29b downregulation (Figure 4). To this end, a commercially available miR-29b inhibitor was repeatedly administered via intraperitoneal (i.p.) injection in non-diabetic +/db mice over 10 weeks. Aortic deposition of the inhibitor was confirmed via a fluorescent label (Figure S1). As expected, miR-29b inhibition induced significant de-repression of target genes *Col1a1* and *Mmp2*. While *Col1a1*

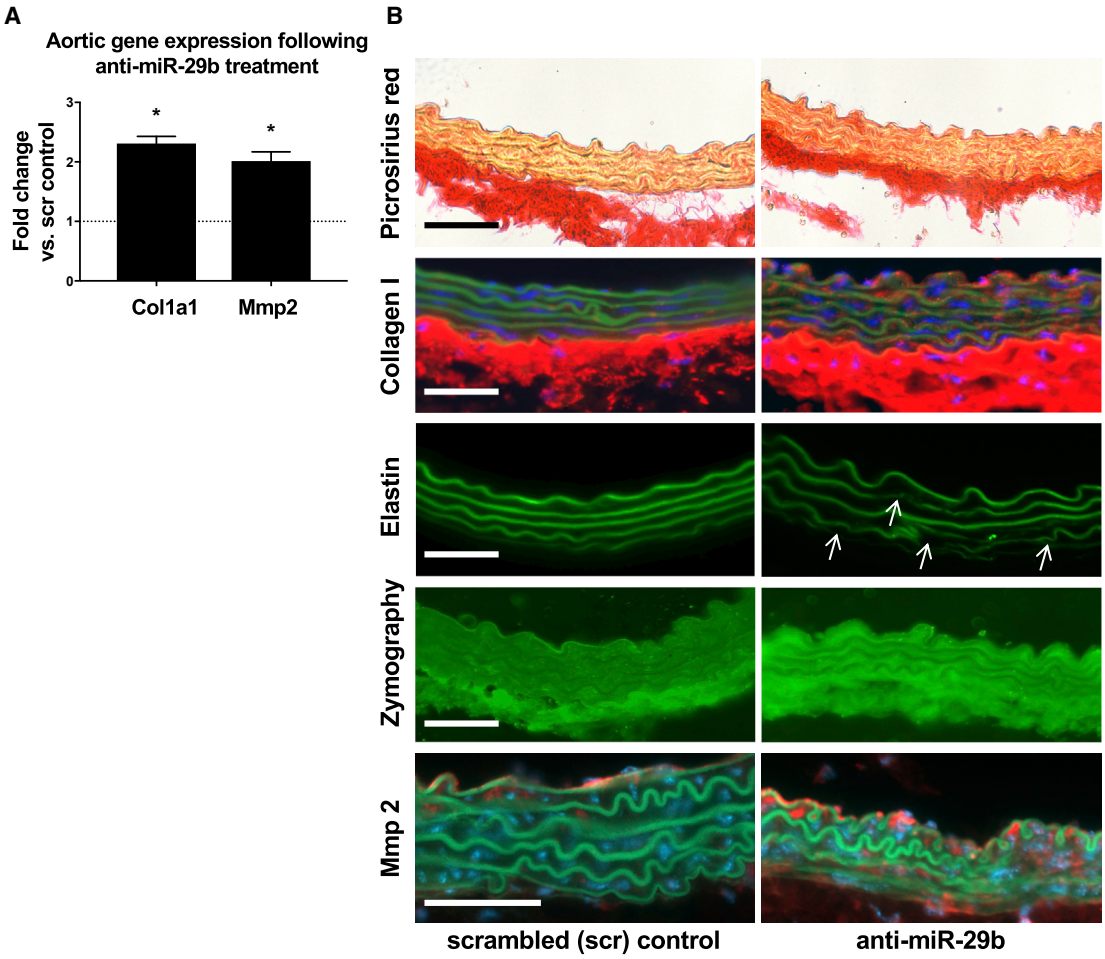

(legend on next page)

upregulation led to increased medial collagen deposition, *Mmp2* upregulation was associated with increased elastolytic activity and enhanced elastin fragmentation. The ECM remodeling induced by miR-29b inhibition was sufficient to significantly increase arterial stiffness (pressure myography and PWV) in +/db mice. Taken together, forced downregulation of miR-29b was sufficient to structurally and functionally recapitulate a diabetic aortic phenotype in non-diabetic mice.

On the cellular level, we found that high glucose stimulation of AoSMCs also induced significant repression of miR-29, which has also been reported for other cell types,[25] and was accompanied by de-repression of *COL1A1* and *MMP2* (Figure 5). Moreover, cellular miR-29b modulation was sufficient to regulate collagen I and MMP2 expression in AoSMCs exposed to normal and high glucose conditions.

While miR-based therapeutic agents have already entered the clinical arena, vascular applications are still largely hampered by poor organ selectivity with resultant off-target effects.[26] We therefore set out to elucidate whether modulation of vascular miR-29b expression was feasible through broader, more readily accessible interventions. Increased ROS abundance in the cardiovascular system is a common feature of T2D, and miR-29b expression has been found to be sensitive to oxidative stress.[2,27] NADPH oxidases belong to the primary ROS-generating enzymes in vessels and, more specifically, are upregulated following the onset of the diabetic phenotype in db/db mice.[28,29] We thus tested the impact of an antioxidant intervention on aortic miR-29b expression, ECM architecture, and arterial stiffness (Figure 6). In line with previous reports, we found increased ROS (superoxide) production in aortic sections from db/db mice, that were significantly reduced by oral antioxidant treatment (TEMPOL).[13,29] We further demonstrated that 10 weeks of TEMPOL treatment significantly increased miR-29b level, accompanied by repression of *Col1a1* and *Mmp2* in db/db aortae. This resulted in attenuated vascular fibrosis and elastin fragmentation and reduced aortic stiffness. Of note, this study may not discern whether the antioxidant effects of TEMPOL treatment on vascular remodeling and stiffening are primarily mediated via miR-29b. Previously, we identified the transcription factor Runx2 to be another redox-sensitive target regulating aortic collagen expression and stiffness in db/db mice.[13] Taken together, our data indicate that diabetic oxidative stress may employ various (partly redundant) signaling pathways (including Runx2, as well as miR-29b; Figure S3) to induce adverse arterial remodeling, thus representing a promising overarching target for intervention.

In conclusion, the present study identifies miR-29b as a comprehensive regulator of aortic remodeling and stiffening in the context of T2D (Figure S3). Thus, we find that through its potential to simultaneously modulate diverse target genes, dysregulation of a single miRNA may in fact orchestrate distinct biological processes (e.g., vascular fibrosis and elastolysis) culminating in a common biological and clinical endpoint (vascular stiffness).

Moreover, this study highlights the detrimental impact of increased oxidative stress as a driver of diabetic arterial stiffening and related cardiovascular complications in this vulnerable patient population. Antioxidant interventions may be effective to limit diabetic arterial stiffening, at least in part though interference with vascular miR-29b-dependent signaling.

From a clinical perspective, our results indicate that interventions aimed at elevating/restoring aortic miR-29b levels in diabetic patients may be beneficial to preserve aortic compliance and maintain physiologic central hemodynamics and dependent end-organ function. However, at the same time, this treatment might potentially suppress local pro-fibrotic reparative mechanisms that may protect T2D patients from AA diseases. Yet, this potential downside may still be outweighed by the net clinical benefit of reducing aortic stiffness as a broad cardiovascular risk factor. Regarding ROS-directed therapy, antioxidant interventions, despite their immense preclinical promise, have unfortunately largely failed to demonstrate comparable clinical benefits in cardiovascular medicine.[30,31] Thus, the identification of powerful downstream redox-sensitive signaling messengers (e.g., miR-29b) may help to design alternative treatment strategies.

MATERIALS AND METHODS

Animals

Male db/db mice (BKS.Cg-Dock7m +/+Leprdb/J) and their age matched heterozygous nondiabetic controls (+/db) were purchased from The Jackson Laboratory (Bar Harbor, ME, USA). Measurements were performed at 10 and/or 20 weeks of age, when db/db mice show significantly elevated blood glucose levels compared to age-matched +/db controls (Figure S2). All animal studies were reviewed and approved by the responsible local animal ethics review boards.

PWV quantification

PWV was assessed as an established *in vivo* marker of aortic stiffness as previously described.[18] In brief, the murine aorta was visualized longitudinally using ultrasound imaging. We then recorded pulse

Figure 4. miR-29b inhibition de-represses extracellular matrix target genes inducing aortic fibrosis, elastin fragmentation, and aortic stiffening

(A) Aortic expression levels of miR-29b target genes Col1a1 and Mmp2 in anti-miR-29b treated +/db mice versus scr controls. Values are mean ± SEM and expressed as fold change relative to the mean expression level in scr controls (=1; dotted line). *p < 0.05 versus +/db. n = 5/group. (B) Representative images of aortic cross sections from 20-week-old mice stained for collagen via picrosirius red (red = collagen) and anti-collagen I immunofluorescence antibody (red = collagen), elastin (autofluorescence of green elastic lamella; arrows exemplarily indicate thinning and breaks), Mmp2 (red), and elastolytic activity (*in situ* zymography). Original magnifications are 400×. Scale bar represents 50 μm. (C) Total collagen content per aortic dry weight. n = 4/group. Values are mean ± SEM. *p < 0.05 versus scr control. (D) Elastin fragmentation index quantified from 3 high-power fields of 5 different aortas per group. Values are mean ± SEM. *p < 0.05 versus scr control. (E) Aortic pressure diameter curves from +/db mice treated with anti-miR-29b versus scr controls. Values are mean ± SEM. *p < 0.05 versus scr controls. (n = 5/group). (F) PWV measurement in +/db mice treated with anti-miR-29b versus scr controls. Values are mean ± SEM. *p < 0.05 versus scr controls. (n = 5/group).

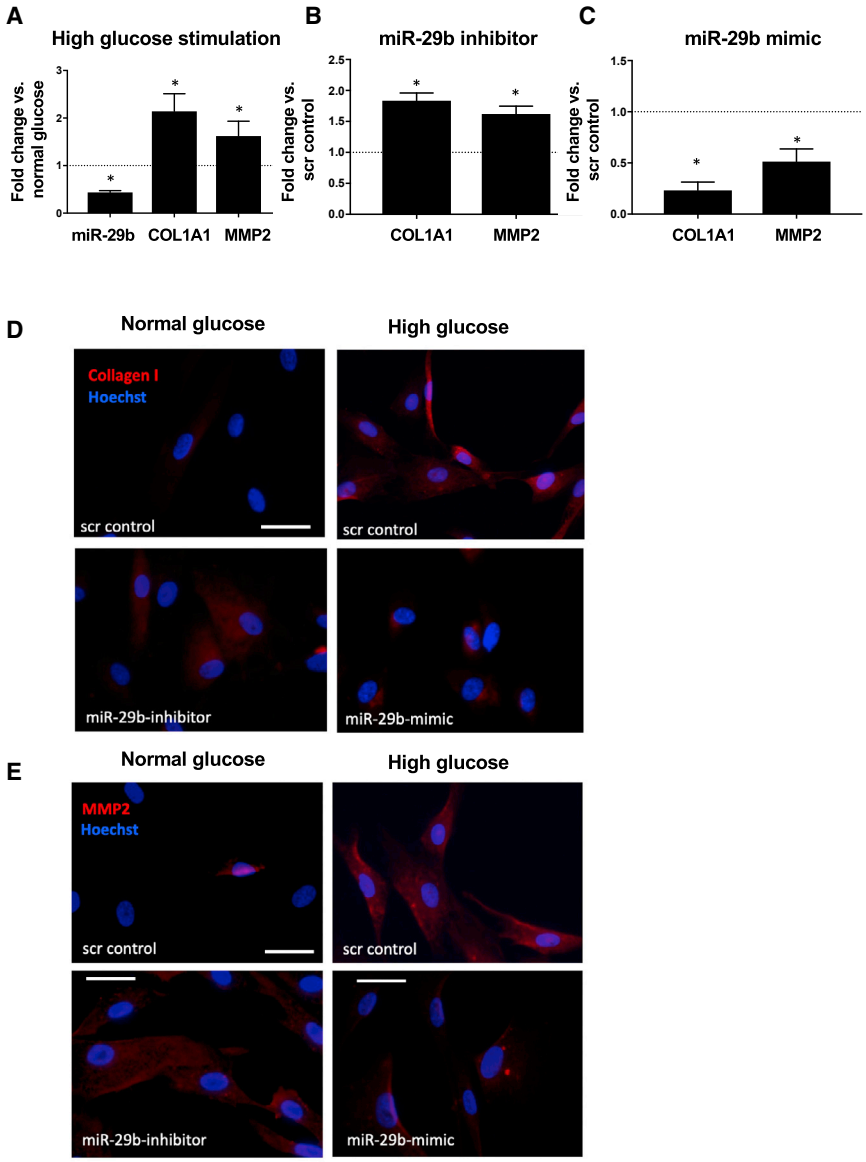

Figure 5. miR-29b expression is downregulated under high glucose conditions in human aortic smooth muscle cells (AoSMCs) and modulates expression of *COL1A1* and *MMP2*

(A) Expression of miR-29b and target genes *COL1A1* and *MMP2* in AoSMCs following high glucose stimulation. Values are mean ± SEM. *p < 0.05 versus normal glucose with osmotic control (n = 4/group). (B) Expression of *COL1A1* and *MMP2* in AoSMCs following treatment with miR-29b inhibitor. Values are mean ± SEM, *p < 0.05 versus scr control (n = 4/group). (C) Expression of *COL1A1* and *MMP2* in AoSMCs following treatment with miR-29b mimic. Values are mean ± SEM, *p < 0.05 versus scr control (n = 4/group). (D) Representative images of AoSMCs stained for collagen I (red). Cells were grown under high glucose and normal glucose conditions (+osmotic control) and treated with miR-29b-inhibitors, -mimics, or scrambled controls as indicated. Nuclei are Hoechst stained (blue). Original magnifications are 400×. Scale bar represents 50 μm. (E) Representative images of AoSMCs stained for MMP2 (red). Cells were grown under high glucose and normal glucose conditions (+osmotic control) and treated with miR-29b-inhibitors, -mimics, or scrambled controls as indicated. Nuclei are Hoechst stained (blue). Original magnifications are 400×. Scale bar represents 50 μm.

waves (via pw-Doppler) at two distinct aortic locations: at the level of the left subclavian artery (LSA) and more distally at the level of the aortic trifurcation (TRF). Using the R-wave of the ECG signal as a time reference, the transit time of the pulse waves between LSA und TRF ($t_{TRF-LSA}$) was calculated. After quantification of the aortic distance between LSA and TRF ($d_{LSA-TRF}$), PWV was calculated as $PWV = d_{LSA-TRF}/t_{TRF-LSA}$.

Pressure myography

Pressure myography was performed to directly assess the passive aortic mechanics *ex vivo* as previously described.[13] In brief, murine thoracic aortae were explanted, placed on specially designed stainless-steel cannulas, and secured with silk surgical suture (10-0). The vessel was mounted in the heated chamber of a pressure arteriograph system (Model 110P, Danish Myotechnology, Copenhagen, Denmark) and stretched to *in vivo* length. Physiological saline solution (PSS) at 37°C, aerated with 5% CO_2/95% O_2, was used to fill the vessel chamber and for aortic perfusion. After 3 preconditioning cycles, the aortic passive pressure-diameter relationship was determined by an automated protocol. The artery was pressurized from 0 to 180 mmHg in 18 mmHg increments, and the vessel's outer diameter was simultaneously tracked by continuous computer video analysis (MyoVIEW software, Danish Myotechnology, Copenhagen, Denmark). The resting diameter d0 was quantified under 0 mmHg intraluminal (transmural) pressure and was not significantly different between the experimental groups tested (d0 ~1,000 μm).

Blood glucose measurements

Blood glucose levels were monitored from tail bleeds taken between 10 a.m. and 12 p.m. using a glucometer (Accu-Check, Roche Diagnostics).

Preparation of mouse aortic tissue for RNA extraction

Mice were sacrificed with an inhalation overdose of isoflurane (Vet One, Meridian, ID, USA). Immediately following sacrifice, the thoracic aorta was transected and flushed via the left ventricle with

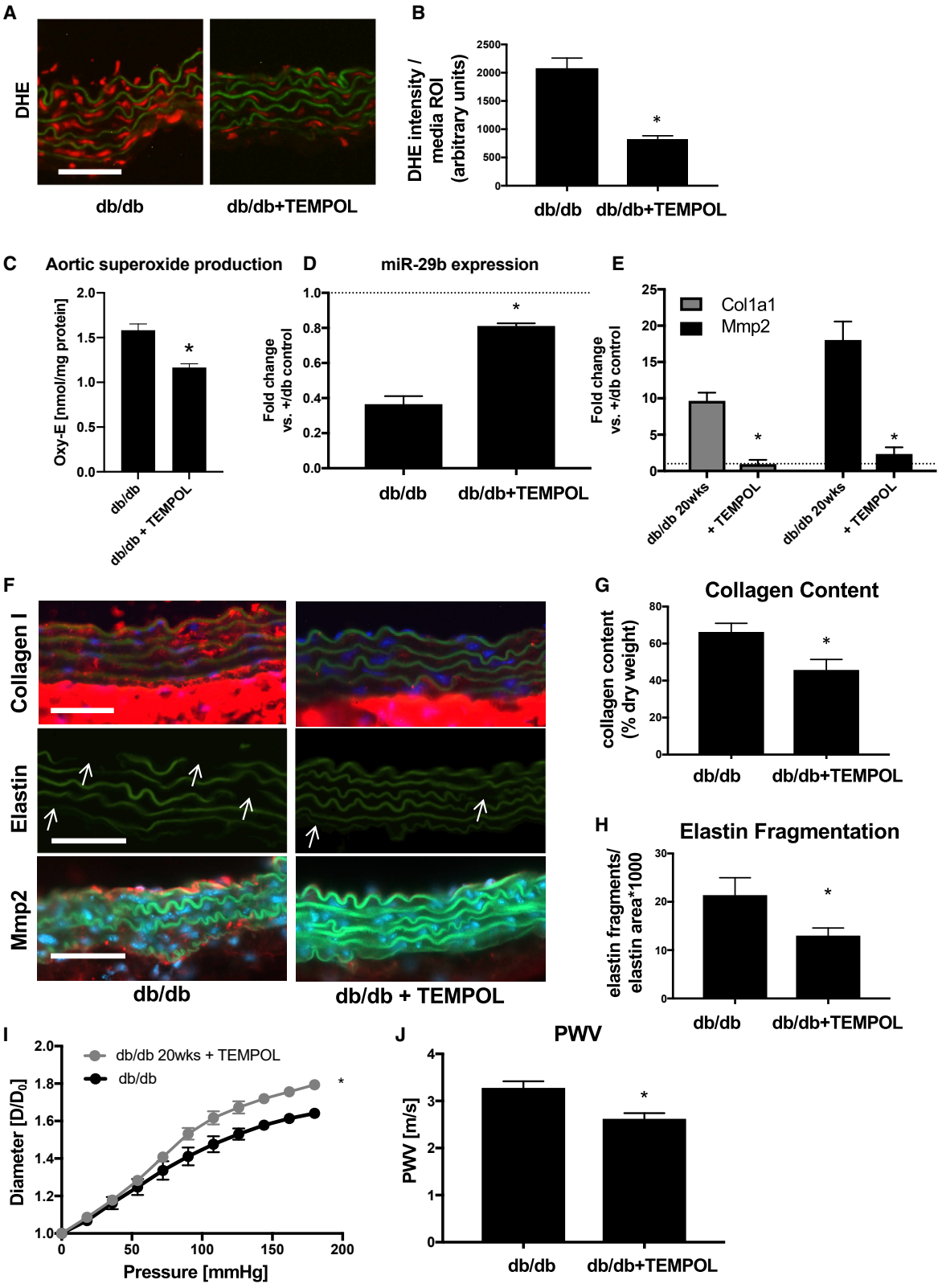

(legend on next page)

ice cold phosphate buffered saline (PBS; pH 7.4). The aorta was then dissected from fat and connective tissue under a microscope (Leica, Wetzlar, Germany). Specimens were snap-frozen in liquid nitrogen and stored at −80°C before further processing.

Human tissue sample acquisition and preparation

Human thoracic aortic samples from diabetic (n = 8) and non-diabetic (n = 8) patients who underwent aorto-coronary bypass surgery (plugs derived from aortic punch biopsy) were collected during surgery, snap-frozen, and stored at −80°C. Groups were matched for age (diabetic patients: 65.00 ± 5.24 years; non-diabetic patients 62.78 ± 5.04 years; p = ns) and smoking status (diabetic patients: 62% smoker; non-diabetic patients: 50% smoker; p = ns).

RNA isolation and quantification

Total RNA was isolated using a TRIzol-based (Invitrogen) RNA isolation protocol. RNA was quantified by Nanodrop (Agilent Technologies), and RNA quality was verified using an Agilent 2100 Bioanalyzer (Agilent Technologies). Samples required 260/280 ratios >1.8, and sample RNA integrity numbers >9 for inclusion. For miRNA analysis, RNA was reverse transcribed using the TaqMan microRNA Reverse Transcription Kit (Applied Biosystems) according to the manufacturer's instructions. MicroRNA and TaqMan Assay Kits (Applied Biosystems) for hsa-miR-29b and sno202 (endogenous control for normalization in mice) and RNU44 (for human samples) were used. For mRNA, the iScript cDNA synthesis kit (Bio-Rad) was used to synthesize first-strand cDNA according to the manufacturer's protocol. TaqMan qRT-PCR assay was performed using mouse and human specific primers for *COL1A1* and *MMP2* (Life Technologies). All probes were normalized to 18S as internal control. Amplification took place on a QuantStudio12K Flex (Applied Biosystems). All fold changes were calculated by the method of ΔΔCt.

Picrosirius red staining

Aortic cross sections (7 μm) were stained using the Picrosirius Red Stain kit (American MasterTech, USA) according to the manufacturer's instructions.

Immunofluorescence (aortic tissue)

Aortic cross sections (7 μm) were incubated with primary antibodies against collagen I and Mmp2 (Abcam) overnight at 4°. Incubation with secondary antibodies (Alexa Fluor 647 goat anti-rabbit; Molecular Probes) was performed for 1 h. Nuclear counterstaining was performed with Hoechst reagent (bisBenzide H 33258; Sigma-Aldrich, St. Louis, MO, USA). Negative controls were performed with the omission of the primary antibody. Imaging was performed using a Leica DM4000B (Buffalo Grove, IL, USA).

Elastin imaging

Elastic lamellae were visualized in aortic cross sections, taking advantage of their green auto-fluorescent properties. Elastin fragmentation was quantified in the histological images using elastin fluorescence morphometric analysis (ImageJ). As previously described,[32] each continuous set of pixels that formed a connected group was defined as an object. An elastin fragmentation index was defined as the ratio of the number of elastin objects to the area of elastin objects. The number of elastin objects was defined by the count of elastin objects within the media region of interest (ROI). The area of elastin objects was equivalent to the total pixel count across all elastin objects within the media ROI.

In situ zymography

In situ zymography was performed with quenched fluorescein (DQ elastin; Invitrogen) as a substrate, which requires cleavage by elastinolytic enzymes to become fluorescent. In brief, aortic sections were exposed to DQ elastin (1 mg/mL; Invitrogen) and 1% agarose solution (ratio 1:10). Representative images were obtained after incubation at 37°C for 24 h.

ISH

ISH for miR-29b was performed by using the miRCURY LNA microRNA ISH Optimization Kit (Exiqon) and 5′-DIG- and 3′-DIG-labeled probes for mmu-miR-29b according to the manufacturer's protocol.

In situ DHE staining

The amount of intracellular ROS production was determined using DHE (Molecular Probes, red fluorescence). Frozen aortic cross

Figure 6. Antioxidant intervention (TEMPOL) restores aortic miR-29b expression and prevents aortic remodeling and stiffening in diabetic mice

(A) *In situ* DHE staining of aortic section from db/db mice, with and without prior TEMPOL treatment. ROS production was indicated by red fluorescence. Original magnification ×400, scale bar, 50 μm. (B) Average DHE intensity was quantified from 3 high power fields of 3 different aortas per group. Values are mean ± SEM. *p < 0.05. (C) Superoxide production in aortic tissue from db/db mice, with and without prior TEMPOL treatment. Superoxide was quantified as the amount of oxidized ethidium (Oxy-E) per milligram protein. Values are mean ± SEM. *p < 0.05 versus db/db without TEMPOL treatment. n = 5/group. (D) miR-29b expression levels in aortae of db/db mice with and without TEMPOL treatment. Values are mean ± SEM and expressed as fold change relative to the mean expression level in +/db controls (=1; dotted line). *p < 0.05 versus db/db without TEMPOL treatment. n = 5/group. (E) Aortic expression levels of miR-29b target genes Col1a1 and Mmp2 in db/db mice with and without TEMPOL treatment. Values are mean ± SEM and expressed as fold change relative to the mean expression level in +/db controls (=1; dotted line). *p < 0.05 versus db/db without TEMPOL treatment. n = 5/group. (F) Representative images of aortic cross sections from 20-week-old mice stained for collagen via anti-collagen I immunofluorescence antibody (red = collagen), elastin (auto-fluorescence of green elastic lamella; arrows exemplarily indicate thinning and breaks), and Mmp2 (red). Original magnifications are 400×. Scale bar represents 50 μm. (G) Total collagen content per aortic dry weight. n = 5/group. Values are mean ± SEM. *p < 0.05 versus db/db without TEMPOL treatment. (H) Elastin fragmentation index quantified from 3 high-power fields of 5 different aortas per group. Values are mean ± SEM. *p < 0.05 versus db/db without TEMPOL treatment. (I) Aortic pressure diameter curves from db/db mice, with and without prior TEMPOL treatment. Values are mean ± SEM. *p < 0.05 versus db/db without TEMPOL treatment (n = 5/group). (J) PWV measurement in db/db mice, with and without prior TEMPOL treatment. Values are mean ± SEM. *p < 0.05 versus db/db without TEMPOL treatment (n = 5/group).

sections (7 μm) were mounted on glass slides, rinsed in PBS, and incubated in 10 μM DHE (37°C, 30 min). Intensity was measured by fluorescence microscopy (Leica DM4000B; Buffalo Grove, IL, USA) using a Texas red filter (488-nm excitation, 610-nm emission). Autofluorescence from elastic lamellae was subtracted, and fluorescence was quantified using ImageJ (National Institutes of Health, Bethesda, MD, USA)

Aortic superoxide quantification (DHE-HPLC)

To evaluate aortic superoxide production, we measured the formation of oxyethidium from DHE using HPLC analysis as previously reported.[29] For each experiment, three 2-mm aortic rings were incubated with 50 μmol/L DHE in fresh Krebs/HEPES buffer and homogenized in 300 μL methanol. Separation of ethidium, oxyethidium, and DHE was performed with the use of an acetonitrile gradient and a C-18 reverse-phase column (Nucleosil 250–4.5 mm) on a Beckman HPLC System. Oxy-E was expressed per milligram protein.

Aortic collagen quantification

Total aortic collagen was quantified using a hydroxyproline-detection based assay (QuickZyme Total Collagen Assay; Quickzyme) as per manufacturer's protocol. In brief, dissected thoracic aortae (n = 5/group) were dried after removal of all loosely attached perivascular connective tissue and dry weight was recorded. Subsequently, aortic tissue was hydrolyzed in 6 M HCl at 95°C for 20 h. In the hydrolysate hydroxypoline content was quantified colorimetrically and correlated to a collagen standard curve. Aortic collagen content was expressed as percentage of dry weight.

In vivo inhibition of miR-29b

For *in vivo* knockdown studies, either a locked nucleic acid (LNA)-carried anti-miR-29b or a scrambled control (scr-miRNA; both from Exiqon) were applied at a concentration of 10 mg/kg via intra peritoneal injection. Treatment of 10-week-old +/db mice was performed once per week over a course of 10 weeks.

Antioxidant treatment

Antioxidant treatment of 10-week-old db/db mice was performed with TEMPOL (1 mmol/L; Sigma Aldrich) in drinking water freshly prepared every other day over a course of 10 weeks.

Cell culture

AoSMCs were propagated in growth media (SmGM-2; Lonza) with 5% fetal bovine serum (FBS) per standard protocols (Lonza; passage number 4–5). Before experimental use, AoSMCs were serum starved for 48 h. For high glucose experiments AoSMCs were incubated in Dulbecco's modified minimal essential medium (DMEM) containing 10% FBS and D-glucose (25 mM for high glucose conditions; 5 mM glucose + 20 mM D-mannitol as osmotic control for normal glucose controls) for 48 h.

In vitro miRNA modulation

miR-29b mimic, miR-29b inhibitor or scrambled (negative control) oligonucleotides (all from Ambion, Thermo Fisher Scientific), were combined with Lipofectamine RNAiMAX (Thermo Fisher Scientific) and applied at 150 pmol/well for a 6-well plate.

Immunofluorescence staining of cells

AoSMCs were cultured in chamber slides under normal glucose or high glucose conditions (see above). The cells were then fixed in 4% paraformaldehyde, washed with PBS, permeabilized with 0.25% Triton-X, and incubated with anti-collagen I and anti-MMP2 antibody (Abcam) overnight at 4°C. The cells were then washed and incubated with secondary antibodies (Alexa Fluor) and Hoechst nuclear counterstain.

Statistics

Data are presented as mean ± SEM. For comparison of 2 groups, Student's t test (two-tailed) was performed; multiple groups (≥ 3 groups) comparison was accomplished by ANOVA with Bonferroni's post-test. For pressure myography analysis, two-way repeated-measures ANOVA was used. Normality and homoscedasticity were tested to ensure that parametric testing was appropriate. A value of $p < 0.05$ (two-sided) was considered statistically significant.

SUPPLEMENTAL INFORMATION

Supplemental Information can be found online at https://doi.org/10.1016/j.omtn.2021.02.021.

ACKNOWLEDGMENTS

This work was supported by research grants from the Deutsche Forschungsgemeinschaft (Sche 2125/2-1 to I.N.S.); the University of Leipzig Medical Faculty (934300-022 to I.N.S.); the University of California Tobacco-Related Disease Research Program (T29IR06360 and 26IP-0041 to J.M.S.); and the German Center for Cardiovascular Research (DZHK) e.V. (81X3300104 to U.R.).

AUTHOR CONTRIBUTIONS

Conception of the study, I.N.S. and U.R.; design, execution, analysis, and interpretation of the experiments, I.N.S., G.C., K.M., A.D., A.P., J.J.-S., J.H., L.M., and U.R.; drafting and editing of the manuscript, I.N.S., M.W., K.M., F.E., A.S., E.S., K.S., J.M.S., and U.R.; funding of the study, infrastructure, I.N.S., J.M.S., M.S., G.H., P.T.S., and U.R.

DECLARATION OF INTERESTS

I.N.S. and U.R. are cofounders of Angiolutions GmbH. Angiolutions GmbH is an academic spin-off company developing vascular devices for aneurysm diseases. The authors declare no competing interests with the contents of this work.

REFERENCES

1. Leon, B.M., and Maddox, T.M. (2015). Diabetes and cardiovascular disease: Epidemiology, biological mechanisms, treatment recommendations and future research. World J. Diabetes *6*, 1246–1258.

2. Kayama, Y., Raaz, U., Jagger, A., Adam, M., Schellinger, I.N., Sakamoto, M., Suzuki, H., Toyama, K., Spin, J.M., and Tsao, P.S. (2015). Diabetic Cardiovascular Disease Induced by Oxidative Stress. Int. J. Mol. Sci. *16*, 25234–25263.

3. Stehouwer, C.D., Henry, R.M., and Ferreira, I. (2008). Arterial stiffness in diabetes and the metabolic syndrome: a pathway to cardiovascular disease. Diabetologia *51*, 527–539.
4. Cruickshank, K., Riste, L., Anderson, S.G., Wright, J.S., Dunn, G., and Gosling, R.G. (2002). Aortic pulse-wave velocity and its relationship to mortality in diabetes and glucose intolerance: an integrated index of vascular function? Circulation *106*, 2085–2090.
5. Lyle, A.N., and Raaz, U. (2017). Killing Me Unsoftly: Causes and Mechanisms of Arterial Stiffness. Arterioscler. Thromb. Vasc. Biol. *37*, e1–e11.
6. Vlachopoulos, C., Aznaouridis, K., and Stefanadis, C. (2010). Prediction of cardiovascular events and all-cause mortality with arterial stiffness: a systematic review and meta-analysis. J. Am. Coll. Cardiol. *55*, 1318–1327.
7. O'Brien, J., Hayder, H., Zayed, Y., and Peng, C. (2018). Overview of MicroRNA Biogenesis, Mechanisms of Actions, and Circulation. Front. Endocrinol. (Lausanne) *9*, 402.
8. Maegdefessel, L., Azuma, J., Toh, R., Deng, A., Merk, D.R., Raiesdana, A., Leeper, N.J., Raaz, U., Schoelmerich, A.M., McConnell, M.V., et al. (2012). MicroRNA-21 blocks abdominal aortic aneurysm development and nicotine-augmented expansion. Sci. Transl. Med. *4*, 122ra22.
9. Schellinger, I.N., Mattern, K., and Raaz, U. (2019). The Hardest Part. Arterioscler. Thromb. Vasc. Biol. *39*, 1301–1306.
10. Raaz, U., Zöllner, A.M., Schellinger, I.N., Toh, R., Nakagami, F., Brandt, M., Emrich, F.C., Kayama, Y., Eken, S., Adam, M., et al. (2015). Segmental aortic stiffening contributes to experimental abdominal aortic aneurysm development. Circulation *131*, 1783–1795.
11. Wolinsky, H., and Glagov, S. (1964). Structural Basis for the Static Mechanical Properties of the Aortic Media. Circ. Res. *14*, 400–413.
12. Wagenseil, J.E., and Mecham, R.P. (2009). Vascular extracellular matrix and arterial mechanics. Physiol. Rev. *89*, 957–989.
13. Raaz, U., Schellinger, I.N., Chernogubova, E., Warnecke, C., Kayama, Y., Penov, K., Hennigs, J.K., Salomons, F., Eken, S., Emrich, F.C., et al. (2015). Transcription Factor Runx2 Promotes Aortic Fibrosis and Stiffness in Type 2 Diabetes Mellitus. Circ. Res. *117*, 513–524.
14. Reddy, G.K. (2004). AGE-related cross-linking of collagen is associated with aortic wall matrix stiffness in the pathogenesis of drug-induced diabetes in rats. Microvasc. Res. *68*, 132–142.
15. Chung, A.W., Yang, H.H., Sigrist, M.K., Brin, G., Chum, E., Gourlay, W.A., and Levin, A. (2009). Matrix metalloproteinase-2 and -9 exacerbate arterial stiffening and angiogenesis in diabetes and chronic kidney disease. Cardiovasc. Res. *84*, 494–504.
16. Sun, H., Zhong, M., Miao, Y., Ma, X., Gong, H.P., Tan, H.W., Zhang, Y., and Zhang, W. (2009). Impaired elastic properties of the aorta in fat-fed, streptozotocin-treated rats. Vascular remodeling in diabetic arteries. Cardiology *114*, 107–113.
17. Song, W., and Ergul, A. (2006). Type-2 diabetes-induced changes in vascular extracellular matrix gene expression: relation to vessel size. Cardiovasc. Diabetol. *5*, 3.
18. Wagenhäuser, M.U., Schellinger, I.N., Yoshino, T., Toyama, K., Kayama, Y., Deng, A., Guenther, S.P., Petzold, A., Mulorz, J., Mulorz, P., et al. (2018). Chronic Nicotine Exposure Induces Murine Aortic Remodeling and Stiffness Segmentation-Implications for Abdominal Aortic Aneurysm Susceptibility. Front. Physiol. *9*, 1459.
19. van Rooij, E., Sutherland, L.B., Thatcher, J.E., DiMaio, J.M., Naseem, R.H., Marshall, W.S., Hill, J.A., and Olson, E.N. (2008). Dysregulation of microRNAs after myocardial infarction reveals a role of miR-29 in cardiac fibrosis. Proc. Natl. Acad. Sci. USA *105*, 13027–13032.
20. Chen, H.Y., Zhong, X., Huang, X.R., Meng, X.M., You, Y., Chung, A.C., and Lan, H.Y. (2014). MicroRNA-29b inhibits diabetic nephropathy in db/db mice. Mol. Ther. *22*, 842–853.
21. Maegdefessel, L., Azuma, J., Toh, R., Merk, D.R., Deng, A., Chin, J.T., Raaz, U., Schoelmerich, A.M., Raiesdana, A., Leeper, N.J., et al. (2012). Inhibition of microRNA-29b reduces murine abdominal aortic aneurysm development. J. Clin. Invest. *122*, 497–506.
22. Wang, H., Guan, X., Tu, Y., Zheng, S., Long, J., Li, S., Qi, C., Xie, X., Zhang, H., and Zhang, Y. (2015). MicroRNA-29b attenuates non-small cell lung cancer metastasis by targeting matrix metalloproteinase 2 and PTEN. J. Exp. Clin. Cancer Res. *34*, 59.
23. Zampetaki, A., Kiechl, S., Drozdov, I., Willeit, P., Mayr, U., Prokopi, M., Mayr, A., Weger, S., Oberhollenzer, F., Bonora, E., et al. (2010). Plasma microRNA profiling reveals loss of endothelial miR-126 and other microRNAs in type 2 diabetes. Circ. Res. *107*, 810–817.
24. Raffort, J., Lareyre, F., Clément, M., Hassen-Khodja, R., Chinetti, G., and Mallat, Z. (2018). Diabetes and aortic aneurysm: current state of the art. Cardiovasc. Res. *114*, 1702–1713.
25. Zhang, J., Wu, L., Chen, J., Lin, S., Cai, D., Chen, C., and Chen, Z. (2018). Downregulation of MicroRNA 29a/b exacerbated diabetic retinopathy by impairing the function of Müller cells via Forkhead box protein O4. Diab. Vasc. Dis. Res. *15*, 214–222.
26. Bartoszewski, R., and Sikorski, A.F. (2019). Editorial focus: understanding off-target effects as the key to successful RNAi therapy. Cell. Mol. Biol. Lett. *24*, 69.
27. Luna, C., Li, G., Qiu, J., Epstein, D.L., and Gonzalez, P. (2009). Role of miR-29b on the regulation of the extracellular matrix in human trabecular meshwork cells under chronic oxidative stress. Mol. Vis. *15*, 2488–2497.
28. Griendling, K.K., Sorescu, D., and Ushio-Fukai, M. (2000). NAD(P)H oxidase: role in cardiovascular biology and disease. Circ. Res. *86*, 494–501.
29. San Martín, A., Du, P., Dikalova, A., Lassègue, B., Aleman, M., Góngora, M.C., Brown, K., Joseph, G., Harrison, D.G., Taylor, W.R., et al. (2007). Reactive oxygen species-selective regulation of aortic inflammatory gene expression in Type 2 diabetes. Am. J. Physiol. Heart Circ. Physiol. *292*, H2073–H2082.
30. Raaz, U., Toh, R., Maegdefessel, L., Adam, M., Nakagami, F., Emrich, F.C., Spin, J.M., and Tsao, P.S. (2014). Hemodynamic regulation of reactive oxygen species: implications for vascular diseases. Antioxid. Redox Signal. *20*, 914–928.
31. Griendling, K.K., Touyz, R.M., Zweier, J.L., Dikalov, S., Chilian, W., Chen, Y.R., Harrison, D.G., and Bhatnagar, A.; American Heart Association Council on Basic Cardiovascular Sciences (2016). Measurement of Reactive Oxygen Species, Reactive Nitrogen Species, and Redox-Dependent Signaling in the Cardiovascular System: A Scientific Statement From the American Heart Association. Circ. Res. *119*, e39–e75.
32. Saatchi, S., Wanchoo, N., Azuma, J., Smith, S.J., Tsao, P.S., Yock, P.G., and Taylor, C.A. (2011). The Use of Immunofluorescent Array Tomography to Study the Three-Dimensional Microstructure of Murine Blood Vessels. Cell. Mol. Bioeng. *4*, 311–323.